Scientific Research Publishing

Journal of Biophysical Chemistry, 2026, 17(1), 1-14
https://www.scirp.org/journal/jbpc
ISSN Online: 2153-0378
ISSN Print: 2153-036X

Alcohol and Its Effects on the Binding of a Catalytically Significant Water Molecule in the Active Site of the Human α-Tubulin Acetyltransferase

Alan Chant[1], Elliott Murray[2], Bennett Harrison-Michaels[1], Christina Kraemer-Chant[2*]

[1]Department of Biochemistry, University of Vermont, Burlington, USA
[2]Department of Chemistry, Saint Michael's College, Colchester, USA
Email: *alan.chant@med.uvm.edu

How to cite this paper: Chant, A., Murray, E., Harrison-Michaels, B. and Kraemer-Chant, C. (2026) Alcohol and Its Effects on the Binding of a Catalytically Significant Water Molecule in the Active Site of the Human α-Tubulin Acetyltransferase. *Journal of Biophysical Chemistry*, **17**, 1-14.
https://doi.org/10.4236/jbpc.2026.171001

Received: January 15, 2026
Accepted: February 24, 2026
Published: February 27, 2026

Abstract

Human alpha-tubulin acetyltransferase 1 (h-αTAT1) is a GNAT-family enzyme responsible for acetylating lysine 40 of α-tubulin, a modification critical for microtubule stability and cellular functions such as intracellular transport and signaling. The enzyme's catalytic activity relies on a well-ordered water molecule coordinated by conserved residues, including Q58, R158, and I64, which facilitate lysine deprotonation and acetyl transfer. Ethanol, a small amphiphilic molecule, is known to interact with proteins by forming hydrogen bonds and hydrophobic contacts, often disrupting structured water networks and altering enzyme dynamics. Although direct ethanol binding to h-αTAT1 has not been reported, previous studies suggest ethanol can inhibit protein function by displacing catalytic water and altering hydrogen bonding networks. Ethanol preferentially binds to hydrophobic residues like isoleucine, especially when located near polar amino acids such as glutamine, a configuration present in h-αTAT1's active site. Chronic ethanol exposure has also been linked to disrupted microtubule acetylation, supporting a possible indirect effect on h-αTAT1 activity. These studies aim to elucidate the structural basis by which ethanol modulates acetyltransferase activity, with broader implications for understanding ethanol-induced cytoskeletal dysfunction. Our results suggest that EtOH has the potential to act as an antagonist and can disrupt the binding of acetyl-CoA to the active site of h-αTAT1. Future molecular dynamics simulations will investigate how ethanol may perturb the substrate-binding cleft of h-αTAT1 and other GNAT-family acetyltransferases such as MEC-17, both with and without acetyl-CoA.

Keywords

Human-Tubulin Acetyltransferase 1 (h-αTAT1), α-Tubulin, Microtubule Stability, Acetyl-CoA, Molecular Dynamics, Pymol, DockingPie

1. Introduction

Alpha-tubulin acetylation plays a crucial role in regulating microtubule stability, intracellular transport, and cellular structure. This post-translational modification is catalyzed by human-tubulin acetyltransferase 1 (h-αTAT1), which acetylates lysine 40 (K40) of α-tubulin [1]. h-αTAT1 belongs to the GNAT (GCN5-related N-acetyltransferase) family and features a conserved GNAT fold that binds acetyl-CoA and facilitates catalysis through a precisely oriented active site [2]. At the core of this mechanism lies a well-ordered water molecule coordinated by conserved residues—especially a glutamine (Q58)—that is activated by a glutamate to serve as a general base, enabling lysine deprotonation and subsequent nucleophilic attack on the acetyl-CoA cofactor [3]. Mutation of Q58 to alanine in h-αTAT1 abolishes catalytic activity, underscoring the central role of this water molecule in enzymatic function.

In addition to Q58, nearby residues such as arginine 158 (R158) and isoleucine 64 (I64) have also been shown to be essential for proper substrate alignment and enzyme function [3]. These residues are involved in a combination of hydrogen bonding and hydrophobic interactions that position α-tubulin for acetylation. Disruption of this carefully orchestrated environment, particularly through displacement of the catalytic water molecule, could compromise enzymatic function. S160 is part of a basic patch crucial for CoA binding; mutation destabilizes protein and impairs function [4].

Ethanol, a small amphiphilic molecule with both hydrophilic (-OH) and hydrophobic character, has the potential to disrupt these finely tuned interactions. It can form hydrogen bonds with polar amino acids and engage in hydrophobic interactions within protein interiors, making it capable of non-specifically binding to a wide range of proteins [5]-[7]. Studies have demonstrated that ethanol can bind preferentially to residues such as isoleucine and those within alpha helices—especially when near glutamine residues—such as the Q58-I64 configuration found in h-αTAT1 [8].

Furthermore, ethanol is known to interfere with catalytically important water molecules, altering hydrogen bonding patterns and potentially causing localized dehydration in active sites [9] [10]. Molecular dynamics simulations have shown that ethanol can displace structured water molecules, resulting in altered protein dynamics and enzyme inhibition even at concentrations as low as 100 mM [6] [9]. Ethanol is also considered a weak, promiscuous binder whose thermodynamic effect—such as increasing system entropy—may favor the displacement of well-ordered water from enzyme active sites [7] [11].

Although no studies have directly demonstrated ethanol binding to h-αTAT1, its known effects on other acetyltransferases and its general physicochemical properties support the hypothesis that ethanol could disrupt the activity of h-αTAT1 by altering the geometry of its substrate-binding cleft and displacing catalytically essential water molecules. These hypotheses are further supported by studies on GNAT-family proteins like MEC-17, where conserved structural and functional features mirror those of h-αTAT1 [3]. Interestingly, isoleucine near glutamine residues has been identified as a preferred ethanol binding motif, further supporting this proposed interaction [6].

Finally, chronic ethanol exposure has been linked to altered microtubule dynamics and acetylation, particularly in neuronal systems [12]. Such alterations could reflect a downstream effect of ethanol's interaction with enzymes like h-αTAT1. Future investigations will utilize molecular dynamics to model ethanol's influence on the active sites of h-αTAT1 and MEC-17, both in the presence and absence of Ac-CoA. Additionally, evidence suggests that ethanol binding is enhanced by hydration, potentially altering protein conformation to favor ethanol association [11]. These dynamics represent a compelling avenue for further research into how ethanol exposure may modulate tubulin acetylation and, by extension, cytoskeletal function.

Many different molecular modeling and docking programs have been developed over the last few years to aid in the visualization and analysis of biomolecular interactions. These include PyMOL and DockingPie, both of which were used in this study. PyMOL is an open-source program that supports high-resolution 3D rendering of protein and ligand structures. It can be used to visually inspect molecular geometry, align structures, measure distances, and analyze binding pockets, among other applications. PyMOL is also useful for structural analysis [13].

DockingPie can be used with PyMOL to streamline molecular docking and automate protein and ligand preparation through determination of protonation state, charge assignment, and energy minimization. It is also useful for binding site specification using coordinates, residue lists, or reference ligands [14]. DockingPie uses docking simulations to generate multiple potential binding interactions, then ranks these interactions (called "poses") using empirical scoring functions and clusters them to highlight preferred binding patterns. DockingPie has been used to dock FDA-approved drugs into SARS-CoV-2 protein targets, with PyMOL employed to visualize key interactions [15]. Similarly, enzyme inhibitor design studies have utilized DockingPie with AutoDock Vina to model the binding of novel acetylcholinesterase inhibitors [16]. In protein engineering, PyMOL is often used to visualize ligand interactions with wild-type and mutant proteins, which can aid in structure-guided mutagenesis [17] [18].

2. Materials and Methods

PyMOL and DockingPie molecular modeling programs were used to visualize and analyze biomolecular interactions of h-αTAT1 with acetyl-CoA, water, and ethanol.

Interpretation of DockingPie Results

Interpreting DockingPie results involves evaluating binding affinity scores, "pose" clustering, receptor-ligand interactions, and potential solvent effects. Docking scores, typically expressed in kcal/mol, reflect predicted binding free energies; a more negative score signifies stronger binding affinity, therefore a more stable and strong interaction. However, these are relative estimates based on approximations from scoring functions [19] [20]. Clustering of similar binding "poses" across multiple runs enhances confidence in these predicted bound structures. The most frequently chosen structures were visualized in PyMOL to assess hydrogen bonding, hydrophobic contacts, π-stacking, and fit of the cofactor or substrate within the binding pocket. For example, in the acetyltransferase h-*α*TAT1, PyMOL was used to identify key interactions such as hydrogen bonding with Q58 and hydrophobic contacts with I64, both of which have been determined to be critical for acetyl-CoA positioning [3].

Root Mean Square Deviation (RMSD) quantifies the average distance between atoms and is typically used to compare a predicted ligand position to a known, acceptable reference structure such as a crystallized complex. RMSD serves as a structural validation tool to assess how accurately a docking prediction mirrors experimental values [21] [22]. In general, RMSD values below 2.0 Å suggest that the docked position can be considered reliable. Values between 2.0 and 3.0 Å are often interpreted as acceptable, with some minor deviation in details. RMSD values of 3.0 Å or higher typically low confidence in the predicted binding mode [23].

In the context of DockingPie, RMSD calculations can be performed directly by comparing docked positions to a reference ligand, often derived from a crystal structure. The software also facilitates visualization of RMSD data through scatter plots of docking affinity (score) versus RMSD, helping users identify positions that are both energetically favorable and structurally accurate [24]. Interpreting such plots can be somewhat complicated; low RMSD values are ideal, as they can indicate close agreement of the predicted binding mode with known binding conformations, but favorable docking scores suggest interactions that are thermodynamically favored. The overarching goal is to optimize both parameters, as this indicates that the resulting position of the ligand in the binding pocket is more likely to be biologically relevant [21] [23] [25].

3. Results

3.1. Analysis of Acetyl-CoA Interactions with h-*α*TAT1

Figure 1 shows the crystal structure of h-*α*TAT1 with acetyl-CoA bound in the active site (PDB Entry - pdb_00004b5o), solved to 1.05 Å resolution. This structure was used as input into DockingPie to determine the amino acids in h-*α*TAT1 that make contact (within 4 Å) to acetyl-CoA. **Figure 2** shows the h-*α*TAT1 sequence with these contacting amino acids highlighted in green. The amino acids are A57, Q58, I121, L122, D123, F124, Y125, I126, Q131, R132, H133, G134, H135, G136, R137, I156, D157, R158, P159, S160, K162, L163, K165, F166, K169, and H170.

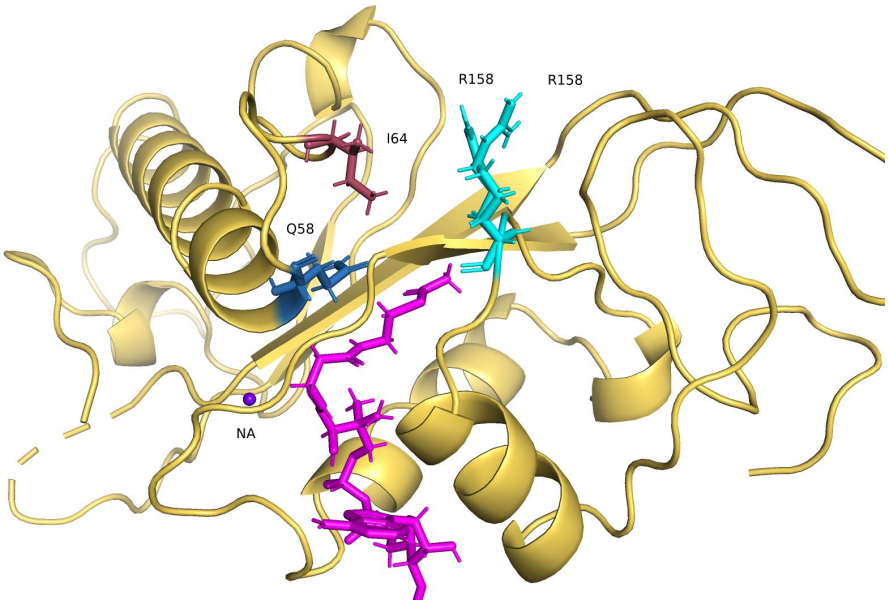

Figure 1. The orientation of acetyl-CoA bound to the active site of h-*α*TAT1 as determined by DockingPie. The three catalytically relevant residues Q58 (blue), R158 (cyan), I64 (red) and acetyl-CoA (magenta) are depicted as stick structures. The associated sodium ion is colored purple.

```
gaasmefpfd vdalfperit vldqhlrppa rrpgtttpar vdlqqqimti idelgkasak
aqnlsapits asrmqsnrhv vyilkdssar pagkgaiigf ikvgykklfv lddreahnev
eplcildfyi hesvqrhghg relfqymlqk ervephqlai drpsqkllkf lnkhynlett
vpqvnnfvif egffahqhrp
```

Figure 2. The h-*α*TAT1 sequence; all the amino acids with which acetyl-CoA makes contact (within 4 Å) are highlighted. The amino acids are A57, Q58, I121, L122, D123, F124, Y125, I126, Q131, R132, H133, G134, H135, G136, R137, I156, D157, R158, P159, S160, K162, L163, K165, F166, K169, and H170.

3.2. Molecular Docking of H_2O with Apo h-*α*TAT1

Molecular docking of H_2O with apo h-*α*TAT1was carried out using DockingPie RxDock. Binding cavities were determined using the Two-Spheres Method in the absence of acetyl-CoA [26]. A single cavity was identified as the active site of the apo h-*α*TAT1 enzyme. **Figure 3** shows the orientation of H_2O within the catalytic region in the active site of apo h-*α*TAT1 as determined by DockingPie RxDoc with the following grid settings: X 38.26, Y 15.82, Z 20.87. **Figure 4** shows the h-*α*TAT1 sequence with all the amino acids with which H_2O is predicted to make contact (within 4 Å) highlighted in pink, as determined by DockingPie. The amino acids are S54, Q58, I64, D123 and F124; three of these (Q58, I64 and R158) have been determined to be required for catalytic activity.

Table 1 shows the RMSD and docking scores that were generated for the 5 most probable orientations within the active site of apo h-*α*TAT1 for H_2O. The average docking score is −10.4198 kcal/mol with a relative standard deviation of 12.6175 kcal/mol. The average RMSD is 44.20 with a relative standard deviation of 2.0. The high RMSD for all the orientations demonstrates a low confidence in any one

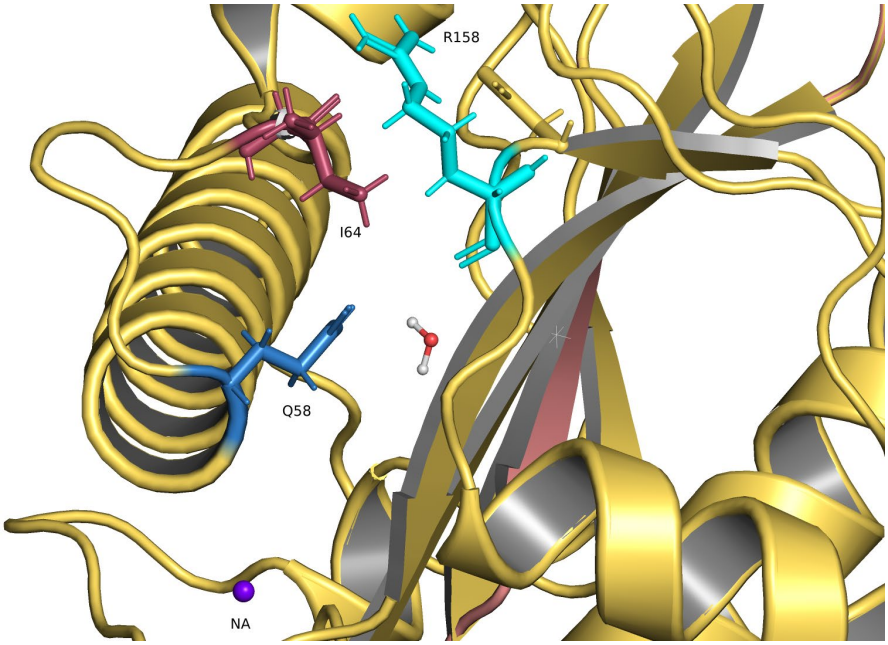

Figure 3. The orientation of H_2O bound to the catalytic region within the active site of apo h-*α*TAT1 as determined by DockingPie. The three catalytically relevant residues Q58 (blue), R158 (cyan) and I64 (red) are depicted as stick structures. The associated sodium ion is colored purple. The H_2O molecule is depicted as a red and white stick and ball structure.

```
gaasmefpfd vdalfperit vldqhlrppa rrpgtttpar vdlqqqimti idelgkasak
aqnlsapits asrmqsnrhv vyilkdssar pagkgaiigf ikvgykklfv lddreahnev
eplcildfyi hesvqrhghg relfqymlqk ervephqlai drpsqkllkf lnkhynlett
vpqvnnfvif egffahqhrp
```

Figure 4. The h-*α*TAT1 sequence with all the amino acids with which H_2O makes contact (within 4 Å) highlighted. The amino acids are S54, Q58, I64, D123, and F124.

Table 1. The RMSD and docking scores (in kcal/mol) of the 5 most probable bound orientations of H_2O within the active site of apo h-*α*TAT1.

NAME	POSE	SCORE	SCORE-inter	SCORE-intra	RMSD Reference: H20
01_obj01_RxDock	1	−10.8196	−3.728	0	43.759
01_obj01_RxDock	2	−10.7261	−4.04207	0	43.77
01_obj01_RxDock	3	−11.6516	−3.68374	0	43.784
01_obj01_RxDock	4	−8.1731	−0.42216	0	43.906
01_obj01_RxDock	5	−10.7284	−3.06235	0	45.802

specific orientation, which may be because water is a simple molecule with less constraints. However, the H_2O docking *location* in proximity to residues Q58, D123, and R158 is consistent with the high-resolution experimental structure, which provides reassurance that the use of the program in further binding analyses is appropriate.

3.3. Molecular Docking of EtOH with Apo h-*α*TAT1

Molecular docking of EtOH with apo h-*α*TAT1 was carried out using DockingPie

RxDock as described above with the following grid setting: X 38.26, Y 15.82, Z 20.87. Binding cavities were determined using the Two-Spheres Method in the absence of acetyl-CoA [26]. A single cavity was identified as the active site of the apo h-αTAT1 enzyme. Docking of EtOH within the cavity placed it near residues Q58, I64 and R158. **Figure 5** shows the orientation of EtOH within the catalytic region in the active site of apo h-αTAT1. **Figure 6** shows the h-αTAT1 sequence with all the amino acids with which EtOH is predicted to make contact (within 4 Å) highlighted in blue. The amino acids are S54, Q58, I64, D123, F124, P159, S160 and L163. It is worth noting that six of these—Q58, D123, F124, P159, S160, and L163—are the same residues that make close contacts with the catalytic water molecule in the crystal structure, and two (Q58 and I64) have been shown to be required for catalytic activity.

Table 2 shows the RMSD and docking scores that were generated for the 5 most probable orientations within the active site of apo h-αTAT1 for EtOH. The average binding docking score is −7.43437 kcal/mol with a relative standard deviation of 17.597 kcal/mol. This is lower than the docking score for the water and the apo protein—an indication that water binds with a higher affinity at the active site when compared to EtOH. The average RMSD is 42.011 with a relative standard deviation of 0.231. As with the docking of water described above, the high RMSD for all the orientations show a low confidence in any one specific orientation, which may be because EtOH is, like water, a simple molecule with less constraints. The significantly lower relative standard deviation of the RMSD values indicate that the precision of the RMSD values is quite a bit higher than it was for the apo protein: water structures. However, the EtOH docking *location* is consistent within the DockingPie results, indicating the precision of docking is high as predicted by the program. The docking location is in proximity to residues Q58, I64 and R158, which are the same residues that make contact to the catalytic bound water molecule.

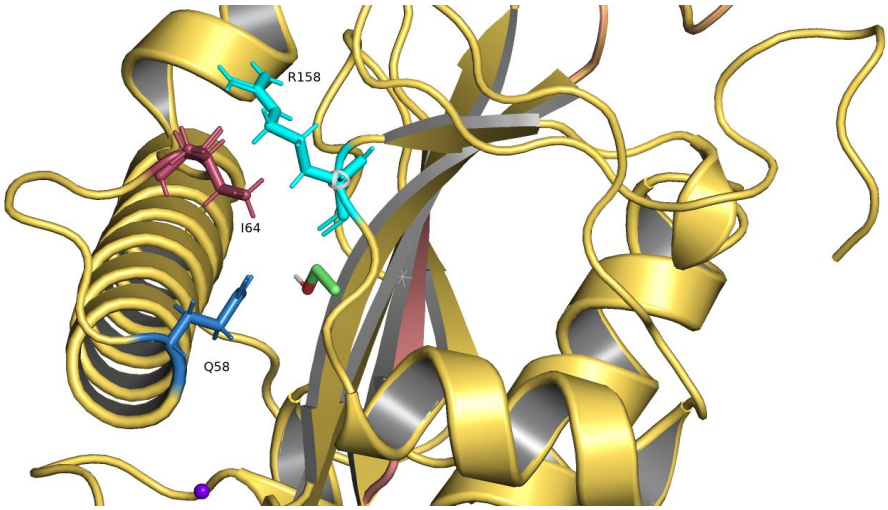

Figure 5. The orientation of EtOH bound to the catalytic region within the active site of apo h-αTAT1 as determined by DockingPie. The three catalytically relevant residues Q58 (blue), R158 (cyan), I64 (red) and acetyl-CoA (magenta) are depicted as stick structures. The associated sodium ion is colored purple. The alcohol molecule is depicted as a red and green stick structure.

```
gaasmefpfd vdalfperit vldqhlrppa rrpgtttpar vdlqqqimti idelgkasak
aqnlsapits asrmqsnrhv vyilkdssar pagkgaiigf ikvgykklfv lddreahnev
eplcildfyi hesvqrhghg relfqymlqk ervephqlai drpsqkllkf lnkhynlett
vpqvnnfvif egffahqhrp
```

Figure 6. The h-*α*TAT1sequence with all the amino acids with which EtOH makes contact (within 4 Å) highlighted. The amino acids are S54, Q58, I64, D123, F124, P159, S160, and L163.

Table 2. The RMSD and docking scores (in kcal/mol) for the 5 most probable bound orientations of EtOH within the active site of apo h-*α*TAT1.

NAME	POSE	SCORE	SCORE-inter	SCORE-intra	RMSD Reference: Alcohol
01_Alcohol_RxDock	1	−7.77066	−4.18051	−3.59015	41.998
01_Alcohol_RxDock	2	−7.87981	−4.34779	−3.53201	41.912
01_Alcohol_RxDock	3	−8.20469	−4.6145	−3.59019	42.003
01_Alcohol_RxDock	4	−8.19727	−4.60781	−3.58947	41.971
01_Alcohol_RxDock	5	−5.11941	−1.9285	−3.19091	42.172

3.4. Comparison of Apo h-*α*TAT1 Docking: H_2O and EtOH

It is important to consider the influence of structured water molecules, which are often excluded from docking studies but can play significant catalytic roles. Solvent effects, including displacement by ethanol or other cosolvents, may alter hydrogen bonding networks; therefore, molecular dynamics simulations are recommended for systems where water plays a structural or functional role [9]-[11].

Based on the RMSD and docking scores, it appears that the binding of water is somewhat more stable than the binding of EtOH, with similar RMSD values. However, when comparing the amino acids with which EtOH and H_2O are predicted to interact in h-*α*TAT1, it is shown that both small molecules make contacts at S54, Q58, I64, D123 and F124. Moreover, EtOH makes additional contacts within a basic region at positions P159, S160 and L163.

3.5. Molecular Docking of Acetyl-CoA with Apo h-*α*TAT1/H_2O

Molecular docking of acetyl-CoA with apo h-*α*TAT1/H_2O was carried out using DockingPie RxDock with the following grid setting: X 34.60, Y 4.24, Z 22.81. Binding cavities were determined using the Reference Ligand Method. A single cavity was identified as the active site of the apo h-*α*TAT1 enzyme. Docking of acetyl-CoA within the cavity placed it near residues Q58, I64 and R158. **Figure 7** shows the orientation of H_2O within the catalytic region in the active site of holo h-*α*TAT1.

Table 3 shows the RMSD and docking scores that were generated for the 5 most probable orientations within the active site of acetyl-CoA with apo h-*α*TAT1/H_2O. The lowest RMSD value out of all 5 orientations is 1.744, which indicates a high level of confidence that that specific orientation (number 5) is the most likely structure. This is also supported by the fact that this orientation has a high negative binding score of −39.6611 kcal/mol.

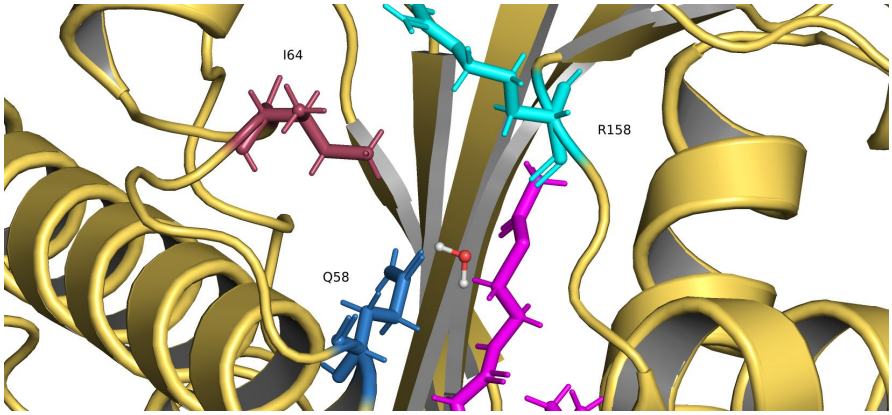

Figure 7. The H_2O and acetyl-CoA (magenta) bound to the active site of h-αTAT1 as determined by DockingPie. The three catalytically relevant residues Q58 (blue), R158 (cyan), I64 (red) are depicted as stick structures and associated sodium ion is colored purple. The H_2O molecule is depicted as a red and white stick and ball structure.

Table 3. The RMSD and docking scores (in kcal/mol) for the 5 most probable bound orientations of acetyl-CoA with apo h-αTAT1/H_2O.

NAME	POSE	SCORE	SCORE-inter	SCORE-intra	RMSD Reference: Acetyl_Coa
01_Acetyl-Coa_RxDock	1	−36.439	−39.8806	5.57703	3.526
01_Acetyl-Coa_RxDock	2	1.42193	−20.411	19.9356	11.156
01_Acetyl-Coa_RxDock	3	−18.3266	−36.5772	13.1356	9.677
01_Acetyl-Coa_RxDock	4	12.8448	−8.52282	14.4889	10.308
01_Acetyl-Coa_RxDock	5	−39.6611	−42.8696	5.35917	1.744

3.6. Molecular Docking of Acetyl-CoA with Apo h-αTAT1/EtOH

Molecular docking of acetyl-CoA with apo h-αTAT1/EtOH was carried out using DockingPie RxDock with the following grid setting: X 34.60, Y 4.24, Z 22.81. Binding cavities were determined using the Reference Ligand Method. A single cavity was identified as the active site of the apo h-αTAT1 enzyme. Docking of acetyl-CoA within the cavity placed it near residues Q58, I64 and R158. **Figure 8** shows the orientation of EtOH within the catalytic region within the active site of holo h-αTAT1.

Table 4 shows the RMSD and docking scores that were generated for the 5 most probable orientations within the active site of acetyl-CoA with apo h-αTAT1/EtOH. Orientation 2 had the lowest RMSD value of 1.904, which indicates a high level of confidence that orientation 2 is the most likely structure. This is also supported by the fact that this orientation has a high negative docking score of −17.4753 kcal/mol.

3.7. Comparison of Acetyl-CoA Docking: Apo h-αTAT1/H_2O and Apo h-αTAT1/EtOH

The RMSD for acetyl-CoA docking with either apo h-αTAT1/H_2O or apo h-αTAT1/EtOH were comparable. However, there is a two-fold difference between

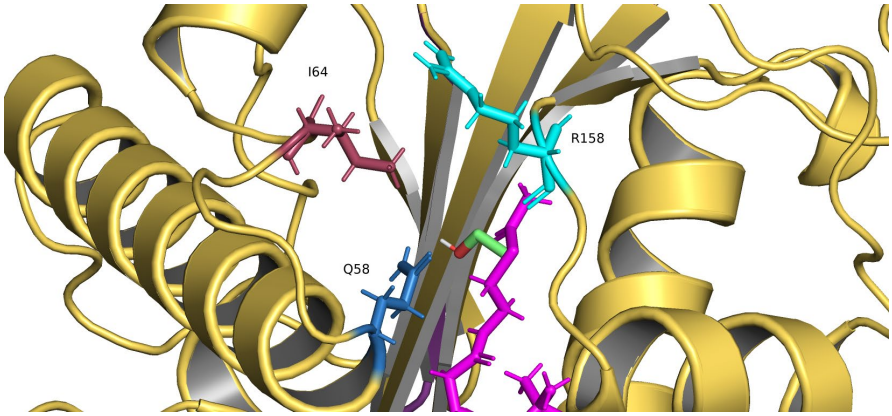

Figure 8. The EtOH and acetyl-CoA (magenta) bound to the active site of h-*α*TAT1 as determined by DockingPie. The three catalytically relevant residues Q58 (blue), R158 (cyan), I64 (red) are depicted as stick structures and associated sodium ion is colored purple. The alcohol molecule is depicted as a red and green stick structure.

Table 4. The RMSD and docking scores (in kcal/mol) for the 5 most probable bound orientations of acetyl-CoA with apo h-*α*TAT1/EtOH.

NAME	POSE	SCORE	SCORE-inter	SCORE-intra	RMSD Reference: Acetyl_Coa	RMSD Reference: Acetyl_Coa
01_Acetyl-Coa_RxDock	1	44.5736	23.9438	18.1105	11.511	11.511
01_Acetyl-Coa_RxDock	2	−17.4753	−21.6793	5.61698	1.904	1.904
01_Acetyl-Coa_RxDock	3	−30.8179	−37.5534	6.04924	2.528	2.528
01_Acetyl-Coa_RxDock	4	−17.2591	−22.0943	2.26319	3.228	3.228
01_Acetyl-Coa_RxDock	5	25.72	3.12149	18.2057	10.773	10.773

the docking score for apo h-*α*TAT1/H_2O with acetyl-CoA (−39.6611 kcal/mol) and apo h-*α*TAT1/EtOH with acetyl-CoA (−17.4753 kcal/mol). Given the less negative binding score for docking of acetyl-CoA with apo h-*α*TAT1/EtOH as compared to the docking of acetyl-CoA with apo h-*α*TAT1/H_2O provides evidence that the presence of the ethanol could potentially *destabilize* binding acetyl-CoA to the apo protein, potentially due to steric hindrance.

4. Discussion and Conclusion

This study proposes a structural and mechanistic framework through which ethanol may influence the function of h-*α*TAT1, a key regulator of microtubule acetylation. Although no direct experimental evidence currently supports ethanol binding to h-*α*TAT1, the convergence of structural features within the enzyme's active site, combined with ethanol's known biochemical behavior, strongly supports a plausible interaction.

Central to h-*α*TAT1's enzymatic activity is a highly conserved catalytic architecture, including residues Q58, R158, and I64, which coordinate a well-ordered water molecule critical for lysine deprotonation and acetyl transfer [3]. Displacement or disruption of this catalytic water, particularly by amphiphilic solvents like ethanol, could impair enzyme function. Ethanol is known to perturb protein func-

tion through hydrogen bonding, hydrophobic interactions, and by altering structured water networks within active sites [9] [10]. This mechanism has been implicated in ethanol-mediated inhibition of other enzymes at relatively low concentrations (~100 mM), where ethanol preferentially associates with alpha-helical regions and hydrophobic residues near polar side chains, such as glutamine and isoleucine [6].

The Q58-I64 configuration in h-αTAT1 represents such a microenvironment. Ethanol's preferential binding to isoleucine residues adjacent to glutamine, as demonstrated in protein structural analyses [8], raises the possibility that ethanol could localize to the active site and perturb the geometry or hydration state necessary for catalysis. Such a disruption may not only block substrate access but also prevent activation of the catalytic water molecule. These hypotheses are reinforced by structural parallels in other GNAT-family acetyltransferases such as MEC-17, which share this glutamine-dependent water-mediated mechanism of catalysis [3].

In addition to direct biochemical interactions, ethanol's systemic effects on microtubule stability further support a functional link to h-αTAT1. Chronic ethanol exposure has been associated with disrupted microtubule acetylation in neurons, leading to cytoskeletal instability and neurotoxicity [12]. These findings suggest that ethanol's physiological impact may stem in part from interference with acetyltransferases like h-αTAT1.

Another significant factor is the role of hydration in modulating ethanol binding. Ethanol is known to exhibit increased affinity for proteins under hydrated conditions, a phenomenon that may facilitate its accumulation near active sites and promote thermodynamically favorable displacement of structured water [7] [11]. This process may irreversibly alter the enzyme's functionality, particularly if catalytically essential water molecules are removed or their hydrogen bonding patterns disrupted.

From these studies, it was determined that a significant difference in the binding of EtOH and H_2O was not predicted by DockingPie when each of these molecules were docked with apo h-αTAT1 (h-αTAT11 in the absence of acetyl-CoA). However, it was observed that, although apo h-αTAT1/EtOH and apo h-αTAT1/H_2O shared five contacts, apo h-αTAT1/EtOH made three additional contacts in the basic region at positions 159, 160 and 163.

Based on the calculated docking energies, it appears that ethanol may in fact destabilize the binding affinity of the acetyl-CoA. If ethanol does indeed destabilize the binding, this effect is almost definitely concentration-dependent, as well as reliant on the binding and release rates of EtOH to the h-αTAT1 protein. Docking energies are preliminary values that do not necessarily indicate that one binding partner is always preferred; water is obviously present at a much higher concentration at the cellular level than EtOH, and this higher concentration might protect against the binding of EtOH and resultant destabilization of the docking of acetyl-CoA. However, these results do indicate that further studies are warranted.

There is a two-fold difference between the predicted docking scores for apo h-αTAT1/H_2O and apo h-αTAT1/EtOH. The less negative docking score for acetyl-CoA with apo h-αTAT1/EtOH could indicate that an incoming acetyl-CoA binds less tightly to h-αTAT1 if the protein has a bound EtOH molecule in the place of the catalytically vital water molecule, potentially due to steric hindrance; the ethanol molecule may in fact destabilize the binding of acetyl-CoA. From these data, we can conclude that EtOH has the potential to act as an antagonist and can disrupt the binding of acetyl-CoA to the active site of h-αTAT11.

5. Future Aims

To elucidate the mechanisms underlying ethanol's impact on h-αTAT1, a comprehensive experimental approach is warranted. Molecular dynamics simulations could be employed to model how ethanol influences the active site conformation, hydration shell, and protein dynamics of h-αTAT1 and other-tubulin transferases in the GNAT family such as MEC-17, both with and without the acetyl-CoA cosubstrate [11] [14]. Complementing these computational studies, site-directed mutagenesis of key residues involved in catalytic water coordination and substrate positioning (Q58, R158, I64) should be conducted, followed by *in vitro* enzymatic assays to assess how these mutations affect acetyltransferase activity in the presence of ethanol [3] [10]. Structural techniques such as X-ray crystallography or cryo-electron microscopy could be utilized to directly visualize ethanol binding and water displacement within the enzyme, with NMR spectroscopy or hydrogen-deuterium exchange mass spectrometry providing additional insight into ethanol-induced changes in protein flexibility and solvent accessibility [2] [5] [9].

To translate these findings to a physiological context, cellular assays measuring microtubule acetylation in cells expressing wild-type or mutant h-αTAT1 under ethanol treatment could be performed [12]. Finally, biophysical techniques such as isothermal titration calorimetry and fluorescence quenching should help to quantify the thermodynamics and affinity of ethanol binding to h-αTAT1, thus elucidating the nature of this weak, promiscuous interaction [7] [11]. This integrative strategy will provide a detailed understanding of how ethanol modulates h-αTAT1 structure and function, potentially advancing knowledge of ethanol-induced cytoskeletal dysfunction.

Conflicts of Interest

The authors declare no conflicts of interest regarding the publication of this paper.

References

[1] Li, L. and Yang, X.J. (2015) Tubulin Acetylation: Responsible Enzymes, Biological Functions and Human Diseases. *Cellular and Molecular Life Sciences*, **72**, 4237-4255. https://doi.org/10.1007/s00018-015-2000-5

[2] Taschner, M., Vetter, I.R. and Lorentzen, E. (2021) Atomic-Resolution Structure of Human α-Tubulin Acetyltransferase Bound to Acetyl-CoA. *Nature Structural & Mo-*

lecular Biology, **28**, 374-382.

[3] Davenport, A.M., Li, Z. and Lorentzen, E. (2023) Structure-Function Relationship of the Human α-Tubulin Acetyltransferase h-αTAT1 and Its Homolog MEC-17. *Journal of Molecular Biology*, **435**, Article 167923.

[4] Davenport, A.M., Collins, L.N., Chiu, H., Minor, P.J., Sternberg, P.W. and Hoelz, A. (2014) Structural and Functional Characterization of the *A*-Tubulin Acetyltransferase MEC-17. *Journal of Molecular Biology*, **426**, 2605-2616. https://doi.org/10.1016/j.jmb.2014.05.009

[5] Howard, R.J., Trudell, J.R. and Harris, R.A. (2011) Structural Insights into Alcohol Modulation of GABA Receptors. *Biochemical Pharmacology*, **81**, 902-910.

[6] Khrustalev, V.V., Barkovsky, E.V., Khrustaleva, T.A. and Khrustaleva, E.A. (2017) Specific Amino Acid Environments as Determinants of Ethanol Binding Sites in Protein Structures. *Journal of Molecular Liquids*, **243**, 340-349.

[7] Wall, M.E., Kim, B. and Mobley, D.L. (2020) Small Molecule Binding to Buried and Solvent-Exposed Sites: Thermodynamic Mechanisms and Applications. *Current Opinion in Structural Biology*, **61**, 88-97.

[8] Khrustalev, V.V., Ruvinsky, A.M. and Khrustaleva, T.A. (2017) Preferential Ethanol Binding to Alpha-Helical Regions and Its Influence on Enzyme Activity. *Protein Engineering, Design & Selection*, **30**, 103-111.

[9] Huang, M., Gabel, S.A. and Kelley, E.E. (2013) Ethanol-Induced Displacement of Catalytic Water Molecules in Enzyme Systems: A Molecular Dynamics Study. *Biophysical Journal*, **105**, 472-481.

[10] Harris, T.K. and Turner, G.J. (2009) Structural Properties of Catalytically Important Water in Enzyme Active Sites. *Biochemistry*, **48**, 3759-3771.

[11] Chong, S.H. and Ham, S. (2015) Impact of Hydration on the Affinity of Alcohol Binding to Proteins: A Molecular Dynamics Study. *The Journal of Physical Chemistry B*, **119**, 6209-6216.

[12] Gibson, M.J., Ma, F. and Thomas, M.A. (2018) Ethanol-Induced Alterations in Microtubule Acetylation and Dynamics in Developing Neurons. *Journal of Neurochemistry*, **146**, 15-27.

[13] Schrödinger, L.L.C. (2015) The PyMOL Molecular Graphics System, Version 2.0.

[14] Wang, M., Li, Y., Gao, J., Zhao, Y. and Lin, Y. (2022) DockingPie: A Modular and Extensible Molecular Docking and Screening Toolkit in Python. *Journal of Cheminformatics*, **14**, Article 68.

[15] Gawriljuk, V.O., Melo-Filho, C.C., Dos Santos, A.S., *et al.* (2021) Identification of Potential SARS-CoV-2 Main Protease Inhibitors Using Molecular Docking, Molecular Dynamics Simulations, and Machine Learning. *Journal of Chemical Information and Modeling*, **61**, 5431-5442.

[16] Khan, S., Hussain, A., AlAjmi, M.F. and Rehman, M.T. (2019) Molecular Docking and Pharmacokinetic Evaluation of Acetylcholinesterase Inhibitors for Alzheimer's Disease. *Current Drug Targets*, **20**, 388-397.

[17] Jumper, J., Evans, R., Pritzel, A., Green, T., Figurnov, M., Ronneberger, O., *et al.* (2021) Highly Accurate Protein Structure Prediction with AlphaFold. *Nature*, **596**, 583-589. https://doi.org/10.1038/s41586-021-03819-2

[18] Whitehead, T.A., Chevalier, A., Song, Y., Dreyfus, C., Fleishman, S.J., De Mattos, C., *et al.* (2012) Optimization of Affinity, Specificity and Function of Designed Influenza Inhibitors Using Deep Sequencing. *Nature Biotechnology*, **30**, 543-548. https://doi.org/10.1038/nbt.2214

[19] Trott, O. and Olson, A.J. (2010) Autodock Vina: Improving the Speed and Accuracy of Docking with a New Scoring Function, Efficient Optimization, and Multithreading. *Journal of Computational Chemistry*, **31**, 455-461. https://doi.org/10.1002/jcc.21334

[20] Forli, S., Huey, R., Pique, M.E., Sanner, M.F., Goodsell, D.S. and Olson, A.J. (2016) Computational Protein-Ligand Docking and Virtual Drug Screening with the AutoDock Suite. *Nature Protocols*, **11**, 905-919. https://doi.org/10.1038/nprot.2016.051

[21] Huang, S. and Zou, X. (2010) Advances and Challenges in Protein-Ligand Docking. *International Journal of Molecular Sciences*, **11**, 3016-3034. https://doi.org/10.3390/ijms11083016

[22] Ferreira, L.G., dos Santos, R.N., Oliva, G. and Andricopulo, A.D. (2015) Molecular Docking and Structure-Based Drug Design Strategies. *Molecules*, **20**, 13384-13421. https://doi.org/10.3390/molecules200713384

[23] Deng, Y., Zheng, Q. and Zhang, X. (2022) Assessing Docking Accuracy Using Root Mean Square Deviation and interaction Fingerprint in Virtual Screening. *Journal of Cheminformatics*, **14**, Article 31.

[24] DockingPie (2024) DockingPie: A PyMOL Plugin for Docking Analysis. GitHub. https://github.com/docking-org/DockingPie

[25] Schneider, G. (2021) Virtual Screening: An Endless Staircase? *Nature Reviews Drug Discovery*, **20**, 1-2.

[26] Rosignoli, S. and Paiardini, A. (2022) DockingPie: A Consensus Docking Plugin for PyMOL. *Bioinformatics*, **38**, 4233-4234. https://doi.org/10.1093/bioinformatics/btac452